ARTICLE

Theoretical Study on Stereodynamics of Reactions of $N(^2D)+H_2 \rightarrow NH+H$ and $N(^2D)+D_2 \rightarrow ND+D$

Xian-fang Yue[a*], Jie Cheng[a], Hai-ran Feng [a], Hong Li[a], Emilia L. Wu[b]

a. Department of Physics and Information Engineering, Ji'ning University, Qufu 273155, China
b. Department of Chemical Engineering and Materials Science, University of Minnesota, 421 Washington Avenue SE, Minneapolis, MN 55455, USA

(Dated: Received on April 1, 2010; Accepted on June 1, 2010)

The vector correlations between products and reagents for the title reactions have been calculated by the quasi-classical trajectory method at a collision energy of 21.32 kJ/mol on an accurate potential energy surface of Ho *et al.* (J. Chem. Phys. **119**, 3063 (2003)). The peaks of the product angular distribution are found to be in both backward and forward directions for the two title reactions. The product rotational angular momentum is not only aligned, but also oriented along the negative direction of y-axis. These theoretical results are in good agreement with recent experimental findings for the two title reactions. The isotopic effect is also revealed and primarily attributed to the difference of the mass factor in the two title reactions.

Key words: Stereodynamics, Quasi-classical trajectory method, Vector correlation, Polarization-dependent differential cross-section, Isotopic effect

I. INTRODUCTION

In recent years, the investigation of the reaction $N(^2D)+H_2(X^1\Sigma_g^+) \rightarrow NH(X^3\Sigma^-)+H(^2S)$ has grown rapidly from both experimental [1−9] and theoretical [10−21] viewpoints, due to its important role in the chemistry of nitrogen containing fuels and nitrogen in the atmosphere [22]. Experimentally, Suzuki *et al.* measured the rate constants for the title reactions by employing a pulse radiolysis-resonance absorption technique at temperatures between 213 and 300 K [1]. They found that the temperature dependence of the rate constants exhibited an Arrhenius behavior. Umemoto *et al.* measured the vibrational and rotational state distributions of the nascent $NH(X^3\Sigma^-)$ and $ND(X^3\Sigma^-)$ molecules formed in the $N(^2D)+H_2$ and $N(^2D)+D_2$ reactions [2−4]. In their experiments, the $N(^2D)$ atoms were generated by two-photon dissociation of NO, while the nascent $NH(X^3\Sigma^-)$ and $ND(\widetilde{X}^3\Sigma^-)$ molecules were detected by laser-induced fluorescence (LIF) technique. They found that the nascent vibrational distributions have $NH(v''=1)/NH(v''=0)=0.8\pm0.1$ and $ND(v''=1)/ND(v''=0)=1.0\pm0.1$, and that the rotational populations of these vibrational states are broad and hot. More recently, Casavecchia *et al.* carried out a series of experimental and theoretical studies on the $N(^2D)+H_2$ and $N(^2D)+D_2$ reactions [5−9]. They have measured the angular and velocity distributions of the nascent NH and ND products in the title reactions under crossed molecular beam (CMB) experiments with mass spectrometric detection technique.

Theoretically, Honvault and Launay carried out the first accurate quantum mechanics (QM) calculations of the $N(^2D)+H_2$ reaction [10] on the PES constructed by Pederson *et al.* [11] with the hyperspherical method. They calculated the vibrationally and rotationally state and resolved integral cross sections at collision energies of 6.69, 10.45, and 15.89 kJ/mol. A forward-backward symmetry was also found in their differential cross sections (DCS) calculations, which indicates that a complex of NH_2 is formed in the reaction. In a recent work, Ho *et al.* improved and refined the PES and developed a more accurate adiabatic ground $1^2A''$ PES [12]. The new PES is fitted by a set of 2715 *ab initio* points resulting from the multireference configuration interaction (MRCI) calculations and a better algorithm. Moreover, the new PES is free of spurious small scale features and is in much better agreement with the *ab initio* calculations, especially in key stationary point regions including the C_{2v} minimum, the C_{2v} transition state, and the N−H−H linear barrier. Employing this new PES, both QM [13−16] and QCT [12, 15−17] calculations have been performed for the title reactions. Most of these studies [12−17] focused on the calculations of the reaction probabilities, integral cross sections, and thermal rate constants. Very few investigations paid attention to the vector properties calculations for the $N(^2D)+H_2$ and $N(^2D)+D_2$ reactions. Vector proper-

*Author to whom correspondence should be addressed. E-mail: xfyuejnu@gmail.com, Tel.: +86-537-3196106. FAX: +86-537-3196037

ties, such as velocities and angular momenta can provide the valuable information about chemical reaction stereodynamics [23, 24]. Therefore, it is necessary to study not only the scalar properties but also the vector properties for fully understanding the dynamics of the title reactions.

In this work, we performed the QCT calculations of the $N(^2D)+H_2$ and $N(^2D)+D_2$ reactions on the more accurate $1^2A''$ state PES by Ho *et al.* [12]. The vector properties and isotopic effects on the title reactions are presented.

II. THEORY

A. Quasi-classical trajectory calculations

The accurate $1^2A''$ state PES constructed recently by Ho *et al.* [12] is employed for the present calculations. The calculation method of QCT is the same as that in Refs.[24–28]. The classical Hamilton's equations are numerically integrated in three dimensions. The collision energy is chosen as 21.32 kJ/mol for both the $N(^2D)+H_2$ and $N(^2D)+D_2$ reactions. The vibrational and rotational levels of the reactant molecules are taken as v=0 and j=0, respectively. A batch of 10^5 trajectories are run for each reaction. The trajectories started at an initial distance of 15 Å between the N atom and the center-of-mass (CM) of the H_2 and D_2 molecules. In classical trajectory calculations, the conservation of the total energy and total angular momentum is very important to guarantee the correctness of trajectories. Especially for the typical insertion reactions $N(^2D)+H_2\rightarrow NH+H$ and $N(^2D)+D_2\rightarrow ND+D$, there is a greater demand for numerical methods with improved accuracy. In previous studies, Schlier *et al.* [29, 30] and Zhang *et al.* [26] introduced tests of some new symplectic integration sixth-order and eighth-order routines applied to the solution of classical trajectories for a triatomic model molecule and its molecular vibrations. These investigators concluded that among a great number of integrator approaches, such as a symplectic integrator of sixth-order and eighth-order, a fourth-order Runge-Kutta initialized fourth-order predictor-corrector integrator, a sixth order predictor-corrector integrator by Gear, the symplectic ones are the most efficient and need the smallest computational expense at a prescribed accuracy level.

In this work, we apply several high-order symplectic integration routines to study the title reactions. The high-order symplectic integrators and their coefficients are taken from Refs.[29, 30], including two sixth-order and three eighth-order algorithms, abbreviated 6a, 6b, 8a, 8b, and 8c. In a given Hamiltonian system whose Hamiltonian can be partitioned, *i.e.*, written as $H=T(p)+U(q)$, we define the derivative terms in the Hamiltonian movement equations as $hq_i=\partial H/\partial p_i$ for the generalized momentum, and $hp_i=-\partial H/\partial q_i$ for the generalized coordinates; let dt be the full time step. Two similar algorithms, algo1 and algo2, differ only by the replacement of p by q, and vice versa. Algo1 can be expressed as [26, 29, 30]

do
i=0, 1, 2, $\cdots$, $n-2$, $n-1$
q=**q**+$dta(2i)$**hq**
p=**p**+$dta(2i+1)$**hp**
end do
q=**q**+$dta(2n)$**hq**

The last step can be concatenated with the first step in a continuing calculation. Then there are $2n$ substeps in every step, where n is 9 for 6a, 8 for 6b, and 17 for 8 series; thus, the number of the calling to the potential derivatives is also n; 6a and 8a must be programmed according to algo1, as presented in Eq.(1), and 6b, 8b, and 8c with algo2, in which p and q are interchanged. The coefficients are defined by $2n+1$ values of $a(i)$, which is taken directly from Refs.[29, 30] without revision. The numerical details of the sixth-order and eighth-order symplectic integrator may be found in the series of articles by Schlier and Seiter [29, 30]. All computations are performed for the title reactions using the same initial conditions based on the PES of Ho *et al.* [12]. The integration step size is chosen to be 0.1 fs. Under these conditions, the calculated total angular momentum is conserved at $>10^{-28}$, and the calculated total energy is conserved at $>10^{-22}$, which is much more precise than required.

B. Polarization-dependent differential cross-sections

The CM frame is used as the reference frame in the present work, which is depicted in Fig.1. The reagent relative velocity vector **k** is parallel to the z-axis. The x-z plane is the scattering plane which contains the initial and final relative velocity vectors **k** and **k′**. θ_t is the angle between the reagent relative velocity and product relative velocity (so-called scattering angle). θ_r and ϕ_r are the polar and azimuthal angles of the final rotational angular momentum **j′**.

The distribution function $P(\theta_r)$ describing the **k**-**j′** correlation can be expanded in a series of Legendre

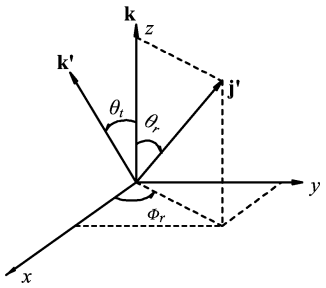

FIG. 1 The center-of-mass coordinate system used to describe the **k**, **k′**, and **j′** correlations.

DOI:10.1088/1674-0068/23/04/381-386

polynomials as [31−33],

$$P(\theta_r) = \frac{1}{2}\sum_k [k] a_0^k P_k(\cos\theta_r) \quad (1)$$

where $[k]$=2k+1, The a_0^k coefficients are given by

$$a_0^k = \langle P_k(\cos\theta_r)\rangle \quad (2)$$

where the angular brackets represent an average over all the reactive trajectories. The expanding coefficients a_0^k are called orientation (k is odd) and alignment (k is even) parameter. In this work, $P(\theta_r)$ is expanded up to k=18, which shows good convergence (10^{-4}).

The dihedral angle distribution function $P(\phi_r)$ describing **k**-**k′**-**j′** correlation can be expanded in Fourier series as [31–33]

$$P(\phi_r) = \frac{1}{2\pi}\left(1 + \sum_{\text{even},n\geq 2} a_n \cos n\phi_r + \sum_{\text{odd},n\geq 1} b_n \sin n\phi_r\right) \quad (3)$$

with a_n and b_n given by

$$a_n = 2\langle \cos n\phi_r\rangle \quad (4)$$

$$b_n = 2\langle \sin n\phi_r\rangle \quad (5)$$

In this calculation, $P(\phi_r)$ is expanded up to n=24, which shows good convergence (10^{-4}). The joint probability density function of angles θ_r and ϕ_r, which determine the direction of **j′**, can be written as

$$P(\theta_r,\phi_r) = \frac{1}{4\pi}\sum_{kq}[k] a_q^k C_{kq}(\theta_r,\phi_r)^* = \frac{1}{4\pi}\sum_k\sum_{q\geq 0}[a_{q\pm}^k \cos q\phi_r - a_{q\mp}^k i\sin q\phi_r]\cdot C_{kq}(\theta_r,0) \quad (6)$$

where $C_{kq}(\theta_r,\phi_r)$ is modified spherical harmonics

$$C_{kq}(\theta_r,\phi_r) = (-1)^q\left[\frac{(k-q)!}{(k+q)!}\right]^{1/2} P_k^q(\cos\theta_r)e^{iq\phi_r} \quad (7)$$

The polarization parameter is evaluated as

$$a_{q\pm}^k = 2\langle C_{k|q|}(\theta_r,0)\cos q\phi_r\rangle,\ k \text{ is even} \quad (8)$$

$$a_{q\pm}^k = 2i\langle C_{k|q|}(\theta_r,0)\sin q\phi_r\rangle,\ k \text{ is odd} \quad (9)$$

In the calculation, $P(\theta_r,\phi_r)$ is expanded up to k=7, which is sufficient for good convergence (10^{-4}).

The full three-dimensional angular distribution associated with **k**-**k′**-**j′** correlation can be represented by a set of generalized polarization-dependent differential cross-sections (PDDCSs) in the CM frame. The fully correlated CM angular distribution is written as [31−34]

$$P(\omega_t,\omega_r) = \sum_{kq}\frac{[k]}{4\pi}\frac{1}{\sigma}\frac{\mathrm{d}\sigma_{kq}}{\mathrm{d}\omega_t}C_{kq}(\theta_r,\phi_r)^* \quad (10)$$

where the angles ω_t=θ_t,ϕ_t and ω_r=θ_r,ϕ_r. σ is the integral cross section. $(1/\sigma)(\mathrm{d}\sigma_{kq})/(\mathrm{d}\omega_t)$ is a generalized PDDCS, and it yields

$$\frac{1}{\sigma}\frac{\mathrm{d}\sigma_{k0}}{\mathrm{d}\omega_t} = 0,\ k \text{ is odd} \quad (11)$$

$$\frac{1}{\sigma}\frac{\mathrm{d}\sigma_{kq+}}{\mathrm{d}\omega_t} = \frac{1}{\sigma}\frac{\mathrm{d}\sigma_{kq}}{\mathrm{d}\omega_t} + \frac{1}{\sigma}\frac{\mathrm{d}\sigma_{k-q}}{\mathrm{d}\omega_t} = 0,\quad k \text{ even and } q \text{ odd or } k \text{ odd and } q \text{ even} \quad (12)$$

$$\frac{1}{\sigma}\frac{\mathrm{d}\sigma_{kq-}}{\mathrm{d}\omega_t} = \frac{1}{\sigma}\frac{\mathrm{d}\sigma_{kq}}{d\omega_t} - \frac{1}{\sigma}\frac{\mathrm{d}\sigma_{k-q}}{\mathrm{d}\omega_t} = 0\quad k \text{ even and } q \text{ even or } k \text{ odd and } q \text{ odd} \quad (13)$$

The PDDCS is written in the following form,

$$\frac{1}{\sigma}\frac{\mathrm{d}\sigma_{kq\pm}}{\mathrm{d}\omega_t} = \sum_{k_1}\frac{[k_1]}{4\pi}S_{kq\pm}^{k_1}C_{k_1-q}(\theta_t,0) \quad (14)$$

where the $S_{kq\pm}^{k_1}$ is evaluated by using the expected value expression to be

$$S_{kq\pm}^{k_1} = \langle C_{k_1q}(\theta_t,0)C_{kq}(\theta_r,0)[(-1)^q e^{iq\phi_r} \pm e^{-iq\phi_r}]\rangle \quad (15)$$

where the angular brackets represent an average over all angles. The differential cross-section is given by

$$\frac{1}{\sigma}\frac{\mathrm{d}\sigma_{00}}{\mathrm{d}\omega_t} = P(\omega_t) = \frac{1}{4\pi}\sum_{k_1}[k_1]h_0^{k_1}(k_1,0)P_{k_1}(\cos\theta_t) \quad (16)$$

The bipolar moments $h_0^{k_1}(k_1,0)$ are evaluated by using the expectation values of the Legendre moments of the differential cross-section and expressed as

$$h_0^{k_1}(k_1,0) = \langle P_{k_1}(\cos\theta_t)\rangle \quad (17)$$

The PDDCS with q=0 is presented by

$$\frac{1}{\sigma}\frac{\mathrm{d}\sigma_{k0}}{\mathrm{d}\omega_t} = \frac{1}{4\pi}\sum_{k_1}[k_1]S_{k0}^{k_1}P_{k_1}(\cos\theta_t) \quad (18)$$

where $S_{k0}^{k_1}$ is evaluated by the expected value expression and given as

$$S_{k0}^{k_1} = \langle P_{k_1}(\cos\theta_t)P_k(\cos\theta_r)\rangle \quad (19)$$

Many photon-initiated bimolecular reaction experiments are sensitive to only those polarization moments with k=0 and k=2. In order to compare calculations with experiments, $(2\pi/\sigma)(\mathrm{d}\sigma_{00}/\mathrm{d}\omega_t)$, $(2\pi/\sigma)(\mathrm{d}\sigma_{20}/\mathrm{d}\omega_t)$, $(2\pi/\sigma)(\mathrm{d}\sigma_{22+}/\mathrm{d}\omega_t)$, and $(2\pi/\sigma)(\mathrm{d}\sigma_{21-}/\mathrm{d}\omega_t)$ are calculated. In the above calculations, PDDCSs are expanded up to k_1=7, which is sufficient for good convergence of 10^{-4}.

DOI:10.1088/1674-0068/23/04/381-386

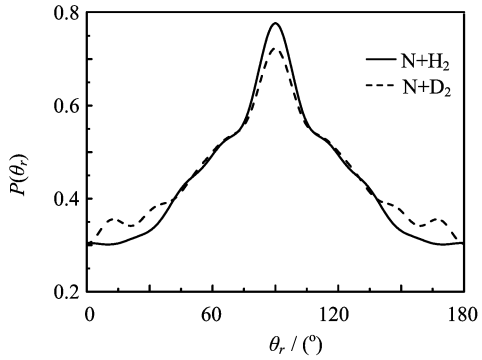

FIG. 2 The angular distribution of $P(\theta_r)$ describing the **k**-**j**′ correlation.

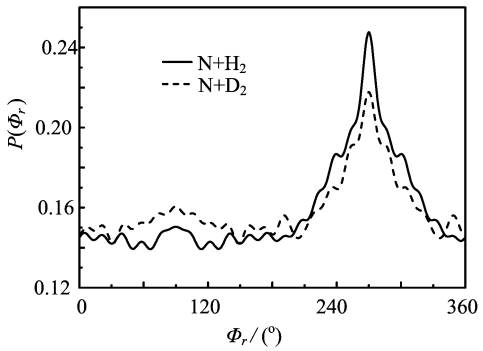

FIG. 3 The dihedral angle distribution of $P(\phi_r)$ describing **j**' with respect to the **k**-**k**' plane.

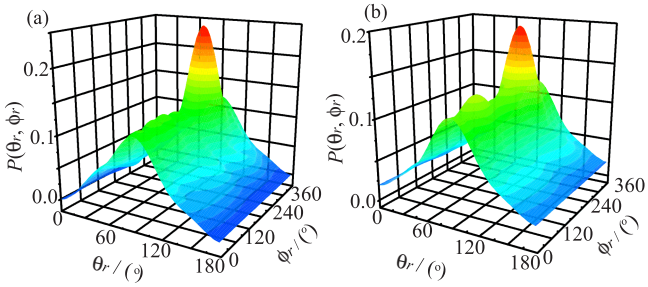

FIG. 4 (a) Polar plots of $P(\theta_r, \phi_r)$ distribution averaged over all scattering angles for the N(^{2}D)+H$_2$→ NH+H reaction. (b) The same as (a) but for the N(^{2}D)+D$_2$→ND+D reaction.

III. RESULTS AND DISCUSSION

Figure 2 displays the calculated $P(\theta_r)$ distributions of the N(^{2}D)+H$_2$→NH+H and N(^{2}D)+D$_2$→ND+D reactions. The product $P(\theta_r)$ distribution describes the **k**-**j**′ correlation. It can be seen from Fig.2 that the $P(\theta_r)$ distribution peaks at θ_r=90°, and exhibits a very good symmetry with respect to 90°. This indicates that **j**′ is strongly aligned along the direction at right angle to the relative velocity direction **k**. The difference of the product distributions in the N(^{2}D)+H$_2$→NH+H reaction and N(^{2}D)+D$_2$→ND+D reaction is clearly shown in Fig.2. The peak of the distribution of the reaction N(^{2}D)+H$_2$→NH+H is broader and higher than that of the reaction N(^{2}D)+D$_2$→ND+D, which indicates that the degree of alignment of the NH product is stronger than that of the ND product. According to the Refs.[27, 35], $P(\theta_r)$ is very sensitive to two factors: one is the character of the PES, and the other is the mass factor (*i.e.* $\cos^2\beta$=$m_A m_B$ /[$(m_A + m_B)(m_B + m_C)$] for the reaction A+BC→AB+C). An increase of mass factor $\cos^2\beta$ will reduce the anisotropic distribution of **j**′ [27, 35]. In our calculations, the same PES is used for the two title reactions. The $\cos^2\beta$ of the N(^{2}D)+H$_2$→NH+H reaction equals to 0.466, and $\cos^2\beta$ of the N(^{2}D)+D$_2$→ND+D reaction is 0.437. Obviously, the $\cos^2\beta$ of the N(^{2}D)+H$_2$→NH+H reaction is larger than that of the N(^{2}D)+D$_2$→ND+D reaction, which is the most likely reason why the distribution of the NH product is broader and higher than that of the ND product.

The dihedral angle distributions $P(\phi_r)$ describes the **k**-**k**′-**j**′ correlations, which is depicted in Fig.3. As shown in Fig.3, the $P(\phi_r)$ distributions exhibit an asymmetry with respect to the **k**-**k**′ scattering plane (or at about ϕ_r=180°), which reflects the strong polarization of the product angular momenta in the two title reactions. The peaks of the $P(\phi_r)$ distributions appear only at ϕ_r= 270°, which means that the rotational angular momentum vectors of the NH and ND products from the two title reactions are oriented along the negative direction of y-axis. It can be obviously seen from Fig.3 that the orientation of the NH product from the N(^{2}D)+H$_2$→NH+H reaction is stronger than that of the ND product from the N(^{2}D)+D$_2$→ND+D reaction.

In order to validate more information about the angular momentum polarization, we plot it in the form of poplar plots θ_r and ϕ_r averaged over all scattering angles in Fig.4. As shown in Fig.4, the $P(\theta_r, \phi_r)$ distributions peak at 90° and 270° for both the NH and ND products from the two title reactions, which are in good accordance with the $P(\theta_r)$ and $P(\phi_r)$ distributions mentioned above. The $P(\theta_r, \phi_r)$ distributions displayed in Fig.4 indicate that the NH and ND products are preferentially polarized in the direction perpendicular to the scattering plane and mainly rotating in planes parallel to the scattering plane.

The generalized PDDCSs describe the **k**-**k**′-**j**′ correlation and the scattering direction of the product molecule. Figure 5 shows the calculated results of the PDDCSs for the N(^{2}D)+H$_2$→NH+H and N(^{2}D)+D$_2$→ ND+D reactions. The PDDCS $(2\pi/\sigma)(d\sigma_{00}/d\omega_t)$ is simply proportional to the differential cross-section (DCS), and only describes the **k**-**k**′ correlation or the product angular distributions. Figure 5(a) displays the $(2\pi/\sigma)(d\sigma_{00}/d\omega_t)$ results of the NH and ND products from the N(^{2}D)+H$_2$→NH+H and N(^{2}D)+D$_2$→ND+D reactions. As apparently shown in Fig.5(a), the product angular distributions peak in both backward and

DOI:10.1088/1674-0068/23/04/381-386

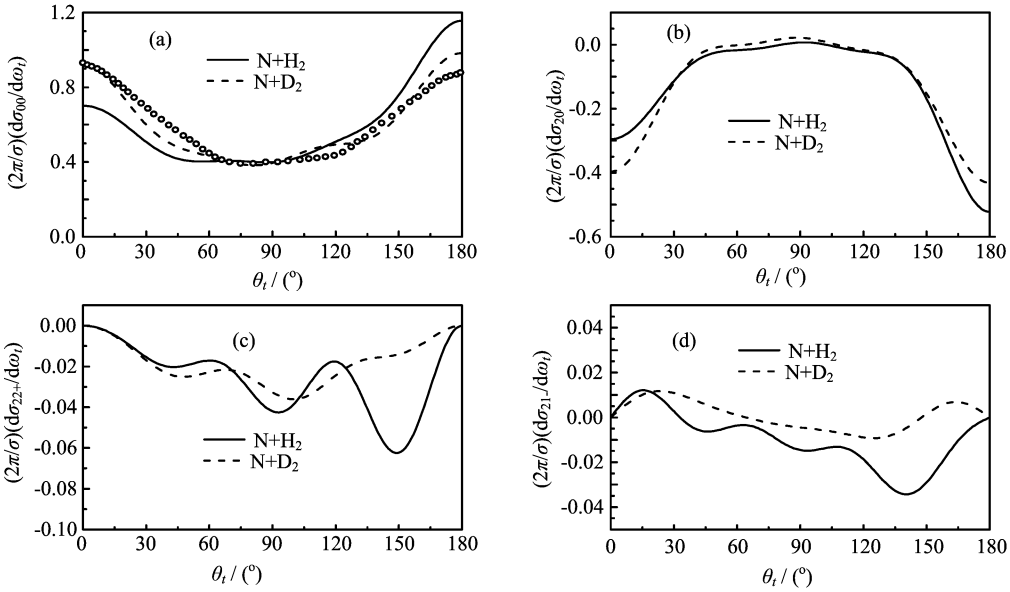

FIG. 5 (a) The PDDCS with (k, q)=(0, 0), and the open circles represent the experimental results of Alagia *et al.* [6]. (b) The PDDCS with (k, q)=(2, 0). (c) and (d) The PDDCS with (k, $q\pm$)=(2, 2+) and (2, 1−), respectively.

forward directions for both the N(^{2}D)+H_2→NH+H and N(^{2}D)+D_2→ND+D reactions. Especially for the N(^{2}D)+D_2→ND+D reaction, the ND product angular distribution is almost backward-forward symmetry. Alagia *et al.* studied the N(^{2}D)+D_2→ND+D reaction using the CMB experimental method [6]. Their experimental results show that the center-of-mass product angular distribution is nearly backward-forward symmetric at the collision energy of 21.32 kJ/mol, which are depicted in Fig.5(a) for comparison. Obviously, our calculated results are in good agreement with the experimental ones of Alagia *et al.* [6]. In contrast to that of the N(^{2}D)+D_2→ND+D reaction, the product angular distributions of the N(^{2}D)+H_2→NH+H reaction are away from the backward-forward symmetry, but peak in backward bias.

The PDDCS $(2\pi/\sigma)(\mathrm{d}\sigma_{20}/\mathrm{d}\omega_t)$ is the expectation value of the second Legendre moment $\langle P_2(\cos\theta_r)\rangle$ and contains the alignment information of $\mathbf{j}'$ with respect to $\mathbf{k}$. As shown in Fig.5(b), the behavior of the $(2\pi/\sigma)(\mathrm{d}\sigma_{20}/\mathrm{d}\omega_t)$ distribution demonstrates an opposite trend to that of the $(2\pi/\sigma)(\mathrm{d}\sigma_{00}/\mathrm{d}\omega_t)$ and obviously depends on the scattering angles. It can be clearly seen from Fig.5(b) that the $(2\pi/\sigma)(\mathrm{d}\sigma_{20}/\mathrm{d}\omega_t)$ values of both the title reactions are negative for both backward and forward scatterings, but they are close to zero for sideways scattering. These results suggest that the $\mathbf{j}'$ is preferentially polarized along the direction perpendicular to $\mathbf{k}$ when the products are scattered forward and backward. In addition, the average values of $\langle P_2(\cos\theta_r)\rangle$ are calculated and found to be −0.400 and −0.378 corresponding to N(^{2}D)+H_2→NH+H and N(^{2}D)+D_2→ND+D reactions respectively, which indicates that the product rotational alignment of NH is stronger than that of ND. This is consistent with the product alignment prediction from the $P(\theta_r)$ distribution shown in Fig.2.

Figure 5 (c) and (d) illustrate the PDDCSs distributions with $q\neq0$. All of the PDDCSs with $q\neq0$ are equal to zero at the extremities of forward and backward scattering. The $(2\pi/\sigma)(\mathrm{d}\sigma_{22+}/\mathrm{d}\omega_t)$ value is positive or negative corresponding to the preference of $\mathbf{j}'$ alignment along the x-axis or y-axis, respectively. It can be seen from Fig.5(c) that the $(2\pi/\sigma)(\mathrm{d}\sigma_{22+}/\mathrm{d}\omega_t)$ values of the title reactions are negative for all scattering angle, which indicates that the alignments of the NH and ND products are preferred along the y-axis. For the N(^{2}D)+H_2→NH+H reaction, the $(2\pi/\sigma)(\mathrm{d}\sigma_{22+}/\mathrm{d}\omega_t)$ displays a stronger polarization at about 150°. Nevertheless, Fig.5(c) exhibits no extremely polarization of the N(^{2}D)+D_2→ND+D reaction as a function of scattering angle. These results mean that the product angular distribution of the N(^{2}D)+D_2→ND+D reaction is more backward-forward symmetric than that of the N(^{2}D)+H_2→NH+H reaction. The PDDCSs $(2\pi/\sigma)(\mathrm{d}\sigma_{21-}/\mathrm{d}\omega_t)$ is related to $\langle\sin^2\theta_r\cos2\phi_r\rangle$, and its distributions are depicted in Fig.5(d). It can be seen from Fig.5(d) that the distributions of the two title reactions are quite different. For the N(^{2}D)+H_2→NH+H reaction, the $(2\pi/\sigma)(\mathrm{d}\sigma_{21-}/\mathrm{d}\omega_t)$ shows a strong polarization at about θ_t=140°. However, the $(2\pi/\sigma)(\mathrm{d}\sigma_{21-}/\mathrm{d}\omega_t)$ shows a slight polarization at about θ_t=25° for the N(^{2}D)+D_2→ND+D reaction. These results indicate that the product angular distributions are anisotropic for both the N(^{2}D)+H_2→NH+H and N(^{2}D)+D_2→ND+D reactions.

DOI:10.1088/1674-0068/23/04/381-386

IV. CONCLUSION

In this work, we have studied the product polarization for the chemical reactions of $N(^2D)+H_2 \rightarrow NH+H$ and $N(^2D)+D_2 \rightarrow ND+D$ by employing the QCT method at the collision energy of 21.32 kJ/mol. The four PDDCSs, $P(\theta_r)$, $P(\phi_r)$, and $P(\theta_r, \phi_r)$ distributions were calculated. The calculated results show that the products mainly tend to be in both backward and forward scattering for the two title reactions. The rotational angular momentum vector $\mathbf{j}'$ of both the NH and ND products from the title reactions is not only aligned, but also oriented along the negative direction of y-axis. These theoretical results are in good agreement with recent experimental findings for the two title reactions. The pronounced isotopic effect is also discussed and principally attributed to the difference of the mass factor in both the title reactions.

V. ACKNOWLEDGMENTS

The authors thank Prof. Ke-li Han for providing stereodynamics QCT code, and thank Dr. T. S. Ho and Prof. H. Rabitz for providing the potential energy surface. This work is supported by the National Natural Science Foundation of China (No.10947103), the Foundation for Outstanding Young Scientist in Shandong Province (No.2008BS01017), and the Young Funding of Jining University (No.2009QNKJ02).

[1] T. Suzuki, Y. Shihira, T. Dato, H. Umemoto, and S. Tsunashima, J. Chem. Soc. Faraday Trans. **89**, 995 (1993).
[2] H. Umemoto and K. Matsumoto, J. Chem. Phys. **104**, 9640 (1996).
[3] H. Umemoto, T. Asai, and Y. Kimura, J. Chem. Phys. **106**, 4985 (1997).
[4] H. Umemoto, N. Terada, and K. Tanaka, J. Chem. Phys. **112**, 5762 (2000).
[5] P. Casavecchia, N. Balucani, M. Alagia, L. Cartechini, and G. G. Volpi, Acc. Chem. Res. **32**, 503 (1999).
[6] M. Alagia, N. Balucani, L. Cartechini, P. Casavecchia, G. G. Volpi, L. A. Pederson, G. C. Schatz, G. Lendvay, L. B. Harding, T. Hollebeek, T. S. Ho, and H. Rabitz, J. Chem. Phys. **110**, 8857 (1999).
[7] N. Balucani, M. Alagia, L. Cartechini, P. Casavecchia, G. G. Volpi, L. A. Pederson, and G. C. Schatz, J. Phys. Chem. A **105**, 2414 (2001).
[8] N. Balucani, L. Cartechini, G. Capozza, E. Segoloni, P. Casavecchia, G. G. Volpi, F. J. Aoiz, L. Bañares, P. Honvault, and J. M. Launay, Phys. Rev. Lett. **89**, 013201-1 (2002).
[9] N. Balucani, P. Casavecchia, L. Bañares, F. J. Aoiz, T. Gonzalez-Lezana, P. Honvault, and J. M. Launay, J. Phys. Chem. A **110**, 817 (2006).
[10] P. Honvault and J. M. Launay, J. Chem. Phys. **111**, 6665 (1999).
[11] L. A. Pederson, G. C. Schatz, T. S. Ho, T. Hollebeek, H. Rabitz, L. B. Harding, and G. Lendvay, J. Chem. Phys. **110**, 9091 (1999).
[12] T. S. Ho, H. Rabitz, F. J. Aoiz, L. Bañares, S. A. Vázquez, and L. B. Harding, J. Chem. Phys. **119**, 3063 (2003).
[13] B. J. Rao and S. Mahapatra, J. Chem. Phys. **127**, 244307 (2007).
[14] S. Y. Lin and H. Guo, J. Chem. Phys. **124**, 031101 (2006).
[15] S. Y. Lin, L. Bañares, and H. Guo, J. Phys. Chem. A **111**, 2376 (2007).
[16] J. F. Castillo, N. Bulut, L. Bañares, and F. Gogtas, Chem. Phys. **332**, 119 (2007).
[17] L. Bañares, F. J. Aoiz, T. González-Lezana, V. J. Herero, and I. Tanarro, J. Chem. Phys. **123**, 224301 (2005).
[18] T. S. Chu, K. L. Han, and A. J. C. Varandas, J. Phys. Chem. A **110**, 1666 (2006).
[19] T. S. Chu, Y. Zhang, and K. L. Han, Int. Rev. Phys. Chem. **25**, 201 (2006).
[20] L. P. Ju, K. L. Han, and J. Z. H. Zhang, J. Comput. Chem. **30**, 305 (2009).
[21] T. S. Chu and K. L. Han, Phys. Chem. Chem. Phys. **10**, 2431 (2008).
[22] A. N. Wright and C. A. Winkler, *Active Nitrogen*, New York: Academic Press, (1968).
[23] M. P. Miranda and D. C. Clary, Chem. Phys. **106**, 4509 (1997).
[24] K. L. Han, G. Z. He, and N. Q. Lou, J. Chem. Phys. **105**, 8699 (1996).
[25] L. M. Raff and D. L. Thompson, *Theory of Chemical Reaction Dynamics*, Boca Raton: CRC Press, 3 (1985).
[26] X. Zhang and K. L. Han, Int. J. Quant. Chem. **106**, 1815 (2006).
[27] M. L. Wang, K. L. Han, and G. Z. He, J. Phys. Chem. A **102**, 20204 (1998).
[28] K. L. Han, L. Zhang, D. L. Xu, G. Z. He, and N. Q. Lou, J. Phys. Chem. A **105**, 2956 (2001).
[29] C. Schlier and A. Seiter, J. Phys. Chem. A **102**, 9399 (1998).
[30] C. Schlier and A. Seiter, Comp. Phys. Commun. **130**, 176 (2000).
[31] M. D. Chen, K. L. Han, and N. Q. Lou, Chem. Phys. **283**, 463 (2002).
[32] M. D. Chen, K. L. Han, and N. Q. Lou, J. Chem. Phys. **118**, 4463 (2003).
[33] J. J. Ma, M. D. Chen, S. L. Cong, and K. L. Han, Chem. Phys. **327**, 529 (2006).
[34] Q. Wei, X. Li, and T. Li, Chin. J. Chem. Phys. **22**, 523 (2009).
[35] M. L. Wang, K. L. Han, and G. Z. He, J. Chem. Phys. **109**, 5446 (1998).

DOI:10.1088/1674-0068/23/04/381-386